A Practical Approach for Static Eccentricity Fault Diagnosis of Hydro-Generators

H. Ehya, *Student Member, IEEE*, A. Nysveen, *Senior, IEEE*, and R. Nilssen

***Abstract*—There has been an increased recognition that more attention needs to be paid to the condition monitoring of hydro-generators to provide a more reliable and sustainable power production. The static eccentricity (SE) fault is one of the prevalent types of failure in the wound rotor synchronous generator that leads to the outage of the power unit. Many different solutions have been proposed for SE fault detection. The techniques are normally based on an offline approach which is not an industry favorite. In this paper, a novel statistical approach is applied to the air gap magnetic field that can detect the fault in its early stage. Furthermore, the severity of the failure on the proposed index in different loading conditions is studied. A polar diagram of the air gap magnetic field is used to detect the location of SE. Finally, the ability of the statistical indices to detect the SE fault in under load variation are verified by experimental results.**

***Index Terms*—Energy level, feature extraction, fault detection, hydro-generator, kurtogram, magnetic field, polar diagram, spectral kurtosis, static eccentricity.**

I. Introduction

Hydro-generators play a pivotal role in the production of electric power. High reliability of power supply depends on the synchronous generators. Online condition monitoring can provide a real-time assessment of the generator. Condition monitoring can detect the gradual aggravating incipient fault in its initial stage before it result in costly damages in the electrical machines.

Different electrical and mechanical faults can occur in a synchronous generator. Mechanical faults may be caused by an unsuited operating condition, mechanical degradation, or defects during the assembly of the machine. The mechanical faults in synchronous machines can be categorized as:

1) Eccentricity
2) Misalignment
3) Broken End Ring
4) Broken Damper Bars
5) Stator Core Deformation

The symptom of mechanical failures may be an unbalanced magnetic field, a sudden increase in the total harmonic distortion in stator voltage or load current, vibration, unbalanced magnetic pull into various parts of the generator.

If the minimum air gap between rotor and stator core varies, then the synchronous generator has a condition which is called eccentricity fault. There are two types of eccentricity: static and dynamic. Static eccentricity is the condition where the shortest length in a nonuniform distribution of the air-gap has a constant length and is fixed in space. In the case of dynamic eccentricity, the air gap length varies in time. Static eccentricity is one of the prevalent faults in synchronous generators. A lower level of eccentricity does not cause any damages to the machines; however, it should be detected at its early stage before the rotor core rubs the stator core and windings.

Over the years, numerous methods have been examined to diagnose static eccentricity fault in the synchronous generators. The SE fault detection based on off-line methods [1] and visual inspection are not the industries favorite-due to two drawbacks:

1) The severity of fault must reach a relatively high level to be discovered, which leads to a significant increase in vibration level. In such a state, further operation of the machine may not be possible anymore.
2) The machine must be stopped and dismantled for few days which leads to an economic loss.

The SE fault detection based on online approaches, like measurements of stator terminal voltage [2], current [3], or variations of machine parameters like inductance [4], has been used to detect eccentricity fault in the synchronous generator. However, these methods can not identify the failure in its early stage since the topology of the rotor or the network harmonic could mask the fault indicators in the mentioned signatures.

In [5], current harmonics like 5^{th}, 7^{th}, 13^{th}, 17^{th}, and 19^{th} is introduced to detect eccentricity fault in the salient pole synchronous generator. These harmonics could detect the eccentricity fault when the minimum air gap reduced up to 85 percent, which is likely close to the rubbing of the stator and rotor. Total harmonic distortion of the generator terminal current is used to detect eccentricity fault under nonlinear load [4]. Neither, can this method detect the fault in its early stage. Besides, the stator and rotor slot shape and rotor saliency have significant effects on the mentioned harmonics that can sometimes even decrease the amplitude of the harmonics due to fault. The same harmonics in the terminal voltage are also used for eccentricity fault detection [4]. The higher-order harmonics are used to detect eccentricity fault; however, the noise signal in the working environment of the power plant could easily mask the higher-order harmonics [4]. The shaft currents and voltages are also introduced to detect eccentricity fault [4]; however, many other faults like

This work was supported by Norwegian Hydropower Centre (NVKS) and Norwegian Research Centre for Hydropower Technology (HydroCen).

Hossein Ehya, Arne Nysveen, and Robert Nilssen are with the Department of Electrical Power Engineering, Norwegian University of Science and Technology (NTNU), 7034 Trondheim, Norway. (e-mail: hossein.ehya@ntnu.no).

978-1-7281-9944-3/20/$31.00 ©2020 IEEE

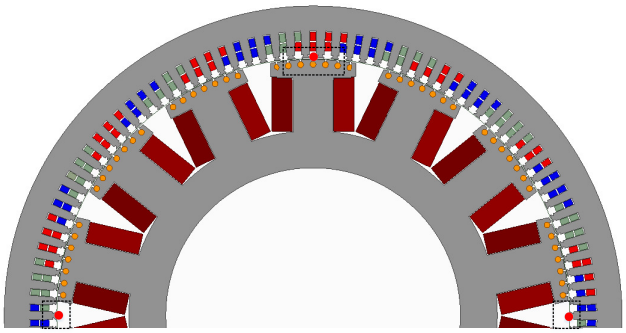

Fig. 1. The finite element model of the wound rotor synchronous generator and the location of the installed hall effect sensor - indicated with a red circle in three points.

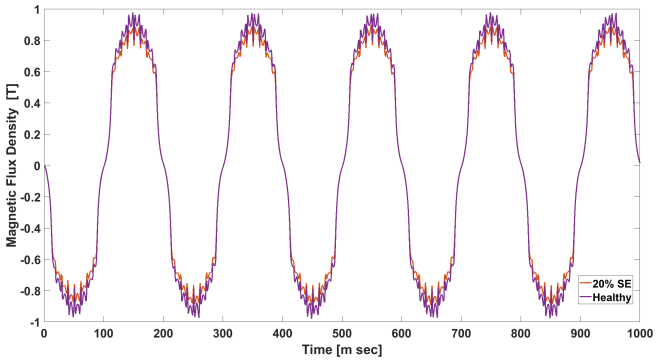

Fig. 2. The air gap magnetic flux density in a healthy and 20% SE fault for a sensor installed in the right measuring point.

a short circuit, dynamic eccentricity, and rotor ground fault also could cause a shaft voltage and current. Consequently, this signal is not a unique indicator of a static eccentricity fault.

In this paper, the magnetic flux density of the air-gap is used to detect static eccentricity fault in the salient pole synchronous generator. The finite element approach is used to simulate the synchronous machine. The location and number of hall-effect sensors that have been installed in the machine's air gap are discussed in order to detect the location of the fault. Although the spectral kurtosis and kurtogram as a statistical tool were used to detect the fault in induction motors successfully, its application to diagnose static eccentricity fault in salient pole synchronous generator by using the magnetic field of the air-gap has not been studied. A novel index is introduced to detect the static eccentricity fault based on the maximum kurtosis and the energy of the spectral kurtosis. The experimental data is used to demonstrate that the proposed indices can precisely detect the healthy and the faulty status of the machine and also the severity of the fault.

II. Finite Element Modeling

A 100-kVA salient pole synchronous generator has been modeled using a two-dimensional finite element approach. The machine was modeled to describe two cases: the healthy case and a case with static eccentricity fault with different levels of severity. The generator is examined at no load and different loading conditions, in constant synchronous speed and with rated current in the rotor field winding. The finite element modeling of the synchronous machine in the healthy case is presented in Fig. 1. The synchronous generator specification is described in Tab. I.

TABLE I
100 kVA, Cosϕ 0.9, 400 V, 14 poles, 428 rpm, Salient Pole Synchronous Generator

Quantity	***Values***	***Quantity***	***Values***
Stator outer diameter	780mm	Stator inner diameter	650mm
No. of slots	114	No. of damper bars/pole	7
No. of turns	8	No. of turns / pole	35
Length of stack	208	Minimum air gap length	1.75mm
Widths of pole shoe	108mm	Widths of pole body	50mm
Widths of stator tooth	8.5mm	Height of stator tooth	29.5mm

A. Location of the sensors

The amplitude of the flux density do not oscillate within a full rotor revolution under static eccentricity fault; however, that is not the case in the rotor field winding inter-turn fault or dynamic eccentricity fault. Static eccentricity gives rise to flux density amplitude variation concerning the position of the sensor; thus, the location of the flux density measuring point is essential. Fig. 1 shows the location of measuring points in the air gap of the synchronous generator - shown as red circles.

The two measuring points are referred to as right and left measurement points, while the other two points are referred to as the top and bottom measuring points. The location of the top and bottom measuring points is assigned at a 90-degree angle with respect to right and left measuring points. Each pair of measuring points must be located on a diametrically opposing side of the synchronous machine in order to experience the same variation of flux density in the concentric and the eccentric conditions. However, the variation of flux density in each of the measuring points may not be the same value due to the configuration of the machine.

There is not any noticeable changes in the flux density in the air gap acquired by sensors if the measuring points are located orthogonal to the orientation of static eccentricity. Consequently, the measured magnetic flux density in the direct axis and the quadrature axis are decoupled, and it could be used to detect the direction of static eccentricity fault. However, with four measuring points that are distributed along the air-gap with a configuration explained above, eccentricity fault must be detected with one pair of measuring points, disregarding the orientation of the failure.

B. Orientation of SE fault

In this paper, the static eccentricity was imposed along the positive x-axis. Fig. 2. presents the variation of the magnetic flux density in the right measuring point in the healthy and under 20% static eccentricity fault. The air-gap length in the right measuring point was increased to 2.1 mm and

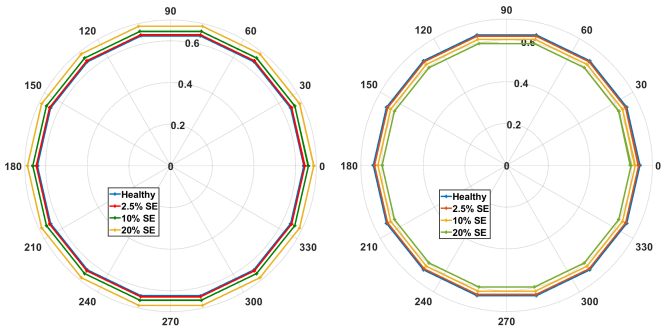

Fig. 3. The average flux density of each pole in a polar diagram, right sensor (right), left sensor (left) - Simulation results.

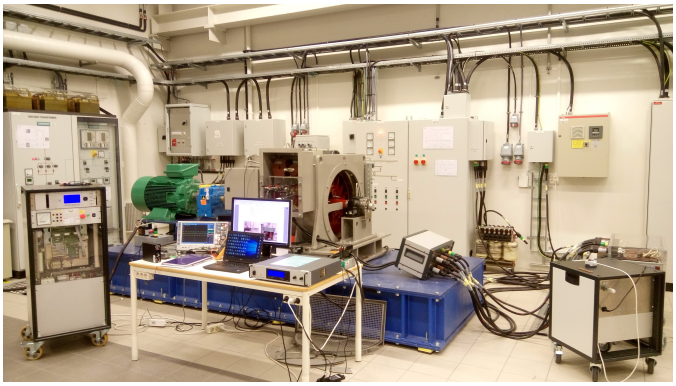

Fig. 4. The experimental test rig of a 100 kVA synchronous generator.

equally decreased in the left measuring point to 1.4 mm. The amplitude of the magnetic flux density in the right measuring point under a given level of static eccentricity decreases in comparison to the healthy case. Since the permeance of the air gap is reduced and with the magnitude of the magneto-motive force similar to the healthy case - this results in a reduction of the air gap magnetic flux density. In order to show the location of the eccentricity fault, the average value of the magnetic flux density of each pole in each measuring point for any number of mechanical revolutions is plotted in a polar diagram, in terms of presenting a larger B_{avg} as a longer vector (radius) in the diagram. Fig. 3. shows such a polar diagram presenting the average flux density, B_{avg}, of each pole - for the right and left measuring points under healthy and eccentricity fault conditions. The radius of the polar diagram for a healthy case in both measuring points is the same. In the case with the SE fault, the B_{avg} of the polar diagram for the right measuring point is decreased, and at the same time, the B_{avg} for the left measuring point is increased. In other words, the length of the air gap on the right side of the machine is increased, which shows the orientation of the SE fault.

The polar diagram of the top and bottom measuring pairs do not show a noticeable variation in their radius in the case of SE fault, which proves the location of the sensors provide the decoupled signals.

III. Experimental Test-Rig

An experimental test rig of a synchronous generator is shown in Fig. 4. This system can be used to measure the air gap magnetic field by hall effect sensors that are installed on stator teeth. The generator windings are star-connected, and the neutral point is grounded. The main parts of the experimental test rig are as below:

1) A 100 kVA salient pole synchronous generator with the specification given in Tab. I.
2) The prime mover of the synchronous machine is a 90 kW induction motor with four poles and rated speed of the 1482 rpm.
3) A gearbox is used to connect the shaft of the induction motor to the synchronous generator.

TABLE II
The Specification of Generator from No-load to Full-load in 4 Different Cases

Characteristics	***No-load***	***Load 1***	***Load 2***	***Load 3***
Output Power	-	30 kW	40 kW	65 kW
Power Factor	-	1.0	0.79	0.93
Exc. Current	56 A	60 A	77 A	84 A
Load Current	-	43 A	56 A	91 A

4) A programmable converter is used to feed the induction motor based on its parameters. The converter is supplied by an external rectifier connected to the network.
5) A 200 kW LAB-HP/E2020 DC power source is used to supply the rotor field winding. The output of the DC power supply is 200 V and 1000 A.
6) Three high precision hall effect sensors (AST244) with the dimensions of $(3.0 \times 5.0 \times 0.8)mm$ installed inside the machine air gap with a flux density to a voltage ratio of 2.54 T/V. The constant DC current supply is used to feed 4.75 mA into the hall-effect sensor.
7) A 16-bit high-resolution oscilloscope, with the sampling frequency of the 20 kHz, is used for sampling purposes.
8) A water-cooled resistor comprised of two parallel sets of resistors, whereas the total resistance can be controlled and adjusted in steps by contactors and relays in a separate control panel. The per-phase resistance could be varied from a maximum of 160 Ω to a minimum of about 2.78 Ω. At the maximum load setting, the dissipated power of the resistors amounts to about 57 kW.
9) Two inductive loads in which each phase are connected in series is connected to the generator by a three-phase transformer. The approximate value of the inductance in each phase based on the turn ratio of the transformer is equal to 22 mH. Table 2 shows the loading condition of the synchronous generator from no load to full load cases.

The static eccentricity fault is created by moving the frame of the machine in both positive and negative directions along the x-axis. In this case, the symmetrical axis of the rotor coincides with its rotation axis but is displaced with respect

to the stator axis. In the same way, the air gap length in the x-axis is not the same anymore, but it is time-invariant. In order to apply a different degree of static eccentricity, four measuring clocks are installed in each moving side of the frame that could measure the required movement precisely.

IV. Fault Detection

The spectral kurtosis (SK) is a useful statistical tool that can demonstrate the non-Gaussian or transient behavior of the time domain signals in the frequency domain [6]. SK can also characterize the location of non-Gaussian components in the frequency domain. Unlike the classical power spectrum density, SK can identify the non-stationary characterization of the signal [7]. Based on the preliminary definition of SK, which is a tool for non-Gaussian signal identification [6], revised the formulation of SK employing Wold-Cramer decomposition and provided a way to discriminate 'conditionally' the non-stationary features of the signal [7] [8]. The kurtosis calculation of each frequency line could recognize the hidden pattern of the non-stationary attribute of the signal. In addition, it is possible to recognize the frequency band that contains the non-stationary signals. Furthermore, additive noise do not, due to the robustness of the method, influence the result of the revised formulation of spectral kurtosis [8].

The measured signals of electrical machines has a non-stationary and transient characteristic in a faulty case which may be detected utilizing the SK approach. The bearing and gearbox faults were detected by using the SK method since the mentioned faults could impose the impulses that are characterized as a non-stationary signal into vibration and current [9] [10].

A. Definition of Kurtosis

Considering b as a random variable, $\kappa(b)$ demonstrate the shape of the probability density function (PDF) that is defined as below [6]:

$$\kappa(b) = \frac{< (b-\mu)^4 >}{\sigma^4} \tag{1}$$

where b represent the air gap magnetic field function, μ and σ are the mean value and standard deviation of b, and $<>$ is a temporal average operator. In order to have a $\kappa(b)$ equal to zero, a standard formulation of $\kappa(b)$ is defined as below [6]:

$$\kappa(b) = \kappa(b) - 3 \tag{2}$$

The coefficient of the $\kappa(b)$ for a Gaussian distribution is zero. It is assumed that the signal of the healthy machine has a Gaussian distribution, and in the case of faulty condition the signals' distribution function is non-Gaussian. In other words, the value of the kurtosis for a healthy machine must be almost zero (since its distribution is Gaussian), which is not the case in reality since the new machine also has some degree of defects like inherent eccentricity. Therefore, any occurrence or increase in the degree of the fault cause the signals deviate from Gaussian distribution and leads to the incremental growth of the kurtosis factor.

B. Spectral Kurtosis

The formal definition of the spectral kurtosis of any zero means conditionally non-stationary random signals in terms of Wold-Cramer formulation is as [7]:

$$b(n) = \int_{-1/2}^{+1/2} H(n,f) e^{j2\pi fn} dZ_b(f) \tag{3}$$

where n is any integer, $dZ_b(f)$ is an orthogonal spectral increment, and $H(n,f)$ is the complex envelope of $b(n)$ at frequency of f. The fourth-order normalised cumulant representation of the spectral kurtosis is expressed as:

$$\kappa_b(f) = \frac{< |H(n,f)|^4 >}{< |H(n,f)|^2 >^2} - 2 \tag{4}$$

where the constant value of 3 in the case of classical kurtosis is replaced by 2 since the $H(n,f)$ is complex function [7]. According to Eq. 4, spectral kurtosis can identify, characterize, and localize the frequency band that contains the hidden transient or non-stationary characteristics in the main signals. The mentioned features of the spectral kurtosis are due to its main properties like [7]:

1) The spectral kurtosis of stationary Gaussian process is zero:
$$\kappa_{(b)}(f) = 0 \tag{5}$$
2) The spectral kurtosis of a stationary process is a constant function of the signal frequency.
$$\kappa_{(b)}(f) = const \tag{6}$$
3) The spectral kurtosis of a conditionally non-stationary process $b(n)$ in a presence of a noise $w(n)$ is
$$\kappa_{(b+w)}(f) = \frac{\kappa_b(f)}{[1+p(f)]^2} \tag{7}$$
where $p(f)$ is the signal to noise ratio as a function of the frequency f.

Although, the spectral kurtosis is a stable tool for signal processing in a sense that is invariant to small changes in its parameters, selection of frequency resolution $\triangle f$ and frequency estimator f have considerable effects on its results. Consequently, the optimal selection of the frequency resolution and the estimator to maximize the spectral kurtosis is crucial to make a representative 'Kurtogram,' which depicts the frequency resolution and frequency in a one plane [11]. The maximum number of kurtogram levels (k) is given by:

$$k = log_2(L) - 7 \tag{8}$$

where L is the number of signal samples. The computational complexity of the kurtogram is equal to the Fast Fourier Transform or wavelet packet.

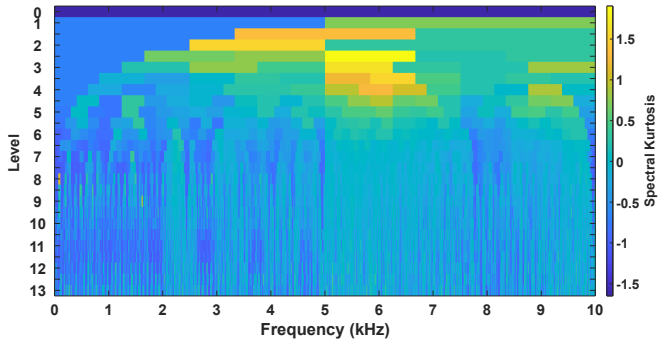

Fig. 5. The kurtogram of a air gap magnetic flux density (left sensor) of the no-load synchronous generator in a healthy case - left sensor. (Experimental result)

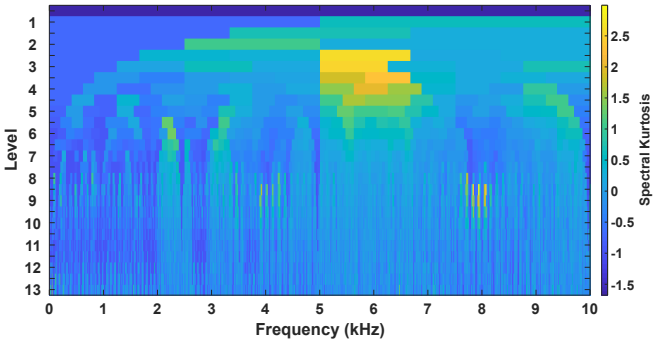

Fig. 6. The kurtogram of a air gap magnetic field (left sensor) of the no-load synchronous generator under 20% SE fault. (Experimental result)

C. Feature extraction

The air gap magnetic flux density measured by hall effect sensors was processed by using spectral kurtosis and kurtogram in different degrees of eccentricity fault under loading condition. The signal was acquired by the sampling frequency of 20 kHz for the duration of 40 seconds, led into a recording length of 200 ksample. The maximum number of levels required for kurtogram, according to Eq. 8, is equal to 13. Two different features based on kurtosis analysis is introduced as below:

1) Maximum kurtosis of the kurtogram
2) Energy of spectral kurtosis

The kurtogram algorithm is applied to the air gap magnetic flux density of the salient pole synchronous generator. Fig. 5 and Fig. 6 show the kurtogram of the synchronous generator in the healthy state and under 20% static eccentricity fault in the no-load case. The same scale similar to Fig. 6. has not been used in Fig. 5 since it reduces its visibility. The intensity of kurtosis levels for the air gap magnetic field under eccentricity fault is varied in comparison to healthy situations, especially from level one up to level five in a different range of frequency bands. The correlation of the maximum kurtosis is also confirmed by the variation since the maximum kurtosis of a 20% SE fault is 2.1, while the maximum kurtosis of a healthy case is 1.9. The proportional relationship between the degree of eccentricity fault and

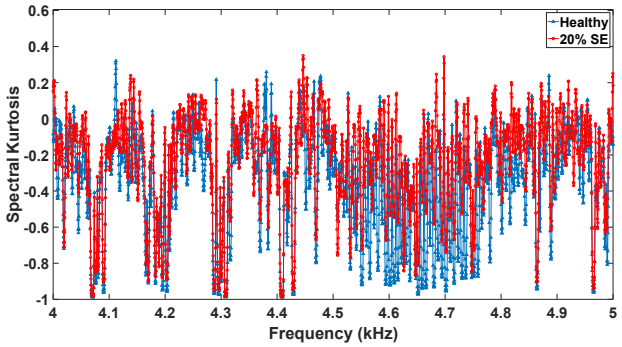

Fig. 7. The spectral kurtosis of a air gap magnetic field (left sensor) for healthy and 20% SE fault for frequency band of 4 kHz to 5 kHz. (Experimental result)

TABLE III
THE MAXIMUM KURTOSIS AMPLITUDE OF A AIR GAP MAGNETIC FIELD IN HEALTHY AND DIFFERENT LEVELS OF SE FAULT

Maximum Kurtosis	***No-Load***	***Load 1***	***Load 2***	***Load 3***
Healthy	1.9	2.2	2.36	2.6
10% SE	2.1	2.3	2.5	2.8
20% SE	3.0	3.2	3.3	3.5

the maximum kurtosis is presented in Tab. III for different loading conditions. The results show that the amplitude of the maximum kurtosis is increased by increasing the severity of the fault. Furthermore, the value of kurtosis's intensity under different loading conditions is different since the magnitude of the air gap magnetic field is changed regarding the load conditions.

Fig. 7 depicts the spectral kurtosis of the air gap magnetic flux density in a healthy and a 20% SE fault for frequency bands between 4 kHz to 5 kHz. The interpretation of spectral kurtosis under healthy and faulty conditions is difficult since the conditional non-stationary signal, due to the fact that the fault signals are scattered in the different time-frequency bands, and in their distribution pattern, is chaotic under a certain level of fault. The physical definition of energy is used to extract the meaningful index that is able to distinguish the fault based on spectral kurtosis. The energy of the kurtosis of the air gap magnetic flux density (b_ϕ) is defined as below:

$$E^{\kappa}_{b_\phi} = \int_{-\infty}^{\infty} |b^{\kappa}(\phi)|^2 \, dt \tag{9}$$

The results from the spectral kurtosis energy analysis for the air gap magnetic flux density are shown in Tab. IV. It is anticipated that the energy levels are sensitive to the occurrence and progression of the fault severity. The amplitude of the energy is decreasing since the magnitude of the air gap magnetic field is decreased with an increased severity of the SE fault. Since the sensor that acquires the data is located on a point which an increased level of eccentricity leads to an increased air gap length and, consequently, a reduction of the magnetic flux density. Results confirm also that the proposed index is sensitive to the fault and thereby can recognize the failure in its early stage.

TABLE IV
THE AIR GAP MAGNETIC FIELD SPECTRAL KURTOSIS ENERGY FOR DIFFERENT SEVERITY OF SE FAULT

Energy (k)	*No-Load*	*Load 1*	*Load 2*	*Load 3*
Healthy	7.18	7.73	7.84	8.08
10% SE	6.68	7.08	7.17	7.37
20% SE	5.46	5.96	6.17	6.35

V. CONCLUSION

In this paper, a practical approach for the detection of static eccentricity fault for salient pole synchronous generator was proposed. The air gap magnetic flux density is found to be sufficiently reliable for the methods presented here and used as the measured signal for signal processing purposes. The location of the installed sensors has significant effects on the fault detection and data acquisition results. Therefore, a detailed explanation is provided to pinpoint the location and required number of sensors. A polar diagram, based on an accurate algorithm, is proposed in order to show the directional orientation of the SE fault. Two novel features of the methods were introduced, in terms of indices, based on the statistical methods called spectral kurtosis and kurtogram. The maximum kurtosis and energy kurtosis of an air gap magnetic flux density is calculated under different severity of the SE fault. The results of the proposed indices show that they have a satisfactory ability to diagnose the severity of the SE fault in its early stage.

VI. ACKNOWLEDGMENT

The authors gratefully acknowledge the contributions of Morten Flå, and Aksel Hanssen for their work on the preparation of the experimental test-rig.

REFERENCES

[1] P. Tavner, L. Ran, J. Penman, and H. Sedding, *Condition monitoring of rotating electrical machines*. IET, 2008, vol. 56.

[2] I. Sadeghi, H. Ehya, and J. Faiz, "Analytic method for eccentricity fault diagnosis in salient-pole synchronous generators," in *2017 International Conference on Optimization of Electrical and Electronic Equipment (OPTIM) 2017 Intl Aegean Conference on Electrical Machines and Power Electronics (ACEMP)*, May 2017, pp. 261–267.

[3] M. Babaei, J. Faiz, B. M. Ebrahimi, S. Amini, and J. Nazarzadeh, "A detailed analytical model of a salient-pole synchronous generator under dynamic eccentricity fault," *IEEE Transactions on Magnetics*, vol. 47, no. 4, pp. 764–771, April 2011.

[4] H. Ehya, I. Sadeghi, and J. Faiz, "Online condition monitoring of large synchronous generator under eccentricity fault," in *2017 12th IEEE Conference on Industrial Electronics and Applications (ICIEA)*, June 2017, pp. 19–24.

[5] H. A. Toliyat and N. A. Al-Nuaim, "Simulation and detection of dynamic air-gap eccentricity in salient-pole synchronous machines," *IEEE Transactions on Industry Applications*, vol. 35, no. 1, pp. 86–93, Jan 1999.

[6] R. Dwyer, "Detection of non-gaussian signals by frequency domain kurtosis estimation," in *ICASSP'83. IEEE International Conference on Acoustics, Speech, and Signal Processing*, vol. 8. IEEE, 1983, pp. 607–610.

[7] J. Antoni, "The spectral kurtosis: a useful tool for characterising non-stationary signals," *Mechanical Systems and Signal Processing*, vol. 20, no. 2, pp. 282 – 307, 2006.

[8] J. Antoni and R. Randall, "The spectral kurtosis: application to the vibratory surveillance and diagnostics of rotating machines," *Mechanical Systems and Signal Processing*, vol. 20, no. 2, pp. 308 – 331, 2006.

[9] S. S. Udmale and S. K. Singh, "Application of spectral kurtosis and improved extreme learning machine for bearing fault classification," *IEEE Transactions on Instrumentation and Measurement*, vol. 68, no. 11, pp. 4222–4233, Nov 2019.

[10] E. Fournier, A. Picot, J. Régnier, M. T. Yamdeu, J. Andréjak, and P. Maussion, "Current-based detection of mechanical unbalance in an induction machine using spectral kurtosis with reference," *IEEE Transactions on Industrial Electronics*, vol. 62, no. 3, pp. 1879–1887, March 2015.

[11] J. Antoni, "Fast computation of the kurtogram for the detection of transient faults," *Mechanical Systems and Signal Processing*, vol. 21, no. 1, pp. 108 – 124, 2007.

VII. BIOGRAPHIES

Hossein Ehya (S'19) received the M.Sc. degree in electrical engineering from the Department of Electrical and Computer Engineering, University of Tehran, Tehran, Iran, in 2013. From 2013 to 2018, Ehya worked as a electrical design engineer in electrical machines companies. He is currently working toward the Ph.D. degree in electrical engineering with Norwegian University of Science and Technology (NTNU), Trondheim, Norway. He is working on electromagnetic analysis and fault detection of synchronous machines. His research intrests include signal processing, pattern recognition, design, modeling, and fault diagnosis of electrical machines.

Arne Nysveen (M'98–SM'06) received his Dr.ing. in 1994 from Norwegian Institute of Technology (NTH). From 1995 to 2002 Nysveen worked as a research scientist at ABB Corporate Research in Oslo, Norway. Since 2002 Nysveen has been a professor at the Norwegian University of Science and Technology (NTNU). He is in charge for the turbine and generator technology research in the Norwegian Research Centre for Hydropower Technology (HydroCen).

Robert Nilssen received his Dr.ing. degree in 1989 from the Norwegian Institute of Technology (NTH). From 1989 to 1996 Nilssen worked at NTH as associated professor. In this period he was scientific advisor for SINTEF. Since 1996 Nilssen has been a professor at the Norwegian University of Science and Technology (NTNU) - with numerical electromagnetic field calculations as his main responsibility. In this period Nilssen has participated in a series of research projects in which design and optimization has been important. Nilssen has also been co-founder of several industry companies. He has been scientific advisor for several companies and in particular for SmartMotor AS and Rolls-Royce Norway - focusing on marine and aviation applications of Permanent Magnet Machines.